NUCLEAR SCIENCE AND ENGINEERING: 82, 429–447 (1982)

Analysis and Modeling of Large-Scale Steam Explosion Experiments

M. L. Corradini*

Sandia National Laboratories, Reactor Safety Studies Division 4441
Albuquerque, New Mexico 87185

Received April 27, 1981
Accepted January 18, 1982

This paper describes current analysis and modeling results of large-scale steam explosion experiments. For the large-scale experiments, a transient one-dimensional explosion model was developed that can qualitatively predict the trends in the experimental data. The model employs a description of vapor film collapse and subsequent fuel fragmentation by thermal and mechanical means. In addition, a simple empirical explosion model was developed and incorporated into a two-dimensional hydrodynamic computer program. This combination can be used to investigate the two-dimensional characteristics of the propagation and expansion phases for large-scale explosions.

I. INTRODUCTION

If a complete failure of normal and emergency coolant flow occurs in a light water reactor (LWR), fission product decay heat would eventually cause the melting of the reactor fuel and the surrounding cladding. In 1975, the Reactor Safety Study[1] concluded that, based on probabilistic risk analysis, LWR core meltdown accidents were the dominant risk contributors to public health and safety. One reason for this conclusion was that containment failure and subsequent radioactivity release were possible given the occurrence of a number of physical processes such as hydrogen combustion, a steam explosion, overpressurization of containment, or core meltthrough of the containment basemat. One of the purposes of the steam explosion program at Sandia National Laboratories is to identify experimentally the magnitudes and time characteristics of pressure pulses and other initial conditions necessary to trigger and to propagate explosive interactions between water and molten materials in an LWR. Recently, a number of experiments were performed[2-6] to aid in accomplishing the first task. The primary purpose of this paper is to present the current results of analysis and modeling that may explain the

*Present address: University of Wisconsin, Department of Nuclear Engineering, Madison, Wisconsin 53706.

[1]"Reactor Safety Study," WASH-1400, U.S. Nuclear Regulatory Commission (1975).

[2]L. S. NELSON and L. D. BUXTON, "Steam Explosion Triggering Phenomena: Stainless Steel and Corium-E Simulants Studied with a Floodable Arc Melting Apparatus," SAND77-0998, NUREG/CR-0122, Sandia National Laboratories (May 1978).

[3]L. S. NELSON et al., "Steam Explosion Triggering Phenomena; Part 2: Corium-A and Corium-E Simulants and Oxides of Iron and Cobalt Studied with a Floodable Arc Melting Apparatus," SAND79-0260, NUREG/CR-0633, Sandia National Laboratories (May 1980).

[4]L. S. NELSON, "Steam Explosion Studies with Single Drops of Molten Refractory Materials," *Proc. Mtg. ANS Thermal Reactor Safety*, Knoxville, Tennessee, April 6-9, 1980, CONF-800403, Vol. I, p. 226, National Technical Information Service (1980).

[5]L. D. BUXTON and W. B. BENEDICK, "Steam Explosion Efficiency Studies: Part I," SAND79-1399, NUREG/CR-0947, Sandia National Laboratories (Nov. 1979); see also W. B. BENEDICK, L. D. BUXTON, and M. L. CORRADINI, "Steam Explosion Efficiency Studies; Part II: Corium Experiments," SAND80-1324, NUREG/CR-1746, Sandia National Laboratories (Oct. 1980).

[6]"LWR Safety Research Program, Quarterly Report," SAND79-2290 (July-Sep. 1979); SAND80-0927 (Oct.-Dec. 1979); SAND80-1304/1 of 4 (Jan.-Mar. 1980); SAND80-1304/2 of 4 (Apr.-June 1980); SAND80-1304/3 of 4 (July-Sep. 1980); SAND80-1304/4 of 4, Sandia National Laboratories (Oct.-Dec. 1980).

experimental observations for large-scale tests and contribute to an understanding of the important phenomena.

Vapor explosions can be thought of as consisting of four phases of energy transfer between the fuel and the coolant:

1. Fuel coolant mixing. The molten fuel and liquid coolant become intermixed, while the heat transfer mode is relatively quiescent (e.g., film boiling).

2. Triggering. The fuel and coolant are brought into near liquid-liquid contact and rapid heat transfer begins.

3. Explosion propagation. The heat transfer process rapidly escalates as more of the fuel is fragmented and as more high-pressure coolant vapor is generated.

4. Expansion. The high-pressure vapor expands against the surroundings with the potential for destructive mechanical work.

During the past few years, over 300 small-scale experiments were performed by Nelson and Buxton[2] using an arc-melter apparatus. In these experiments, molten material (stainless steel, Corium-A, Corium-E, and iron oxide) held on a copper hearth was flooded with water, and an explosion was triggered by firing an exploding wire. Recently, Nelson et al.[3] have begun a series of single droplet experiments where a molten droplet is injected into a water bath and a spontaneous or triggered explosion occurs. Previous analyses[7] of the triggering phase of these experiments suggested that the experimental initial conditions (coolant temperature, ambient pressure, and molten fuel composition) could make the triggering of the explosion more difficult; however, if the trigger were increased in strength, the explosion could again be induced.

Large-scale experiments were originally conducted by Buxton and Benedick[5] in an open chamber using an iron aluminum oxide fuel simulant and Corium-A. Recently, Mitchell began the fully instrumented test series[6] (FITS). The FITS experiments allow explosions to be conducted in a closed vessel so that all post-test explosion debris can be collected. This paper reviews the results of these latter large-scale tests and analyzes the explosion propagation and expansion phases using newly developed models.

[7]M. L. CORRADINI, "Phenomenological Modelling of the Small-Scale Vapor Explosion Experiments," SAND79-2003, NUREG/CR1105, Sandia National Laboratories (Feb. 1980).

II. OPEN GEOMETRY EXPERIMENTS

During the last two years, Buxton and Benedick conducted a series of steam explosion experiments[5] to determine the conversion ratio[8] of the fuel thermal energy into mechanical work at a large scale (5- to 20-kg fuel mass). The tests were designated "open geometry" experiments because they were intended to be scoping in nature, performed in an open vessel with minimal instrumentation. Over 60 experiments were conducted using thermitically[9] generated iron/aluminum oxide, Fe-Al_2O_3, and Corium-A+R (Ref. 10). The fuel simulant, Fe-Al_2O_3, was used in the majority of tests (50) because it is a reasonable simulant for the Corium melts: in addition to being nonhazardous, it was very inexpensive and easy to produce. The fuel mass delivered into the water was, on the average, between 10 and 20 kg, many orders of magnitude larger than that used in small-scale tests.[1-3] The experiments were conducted in an open vessel (Fig. 1). The fuel melt was thermitically generated in an insulated cylinder held above the water tank, and the melt was then poured into the water. The mechanical work generated by the explosion was determined by measuring the impulse delivered downward to crushable honeycomb blocks and by estimating the potential energy of the upward ejected debris (water and fuel). A summary of the experimental results is given in Table I.

II.A. Effect of Initial Conditions

II.A.1. Coolant Temperature

Four experiments were conducted with the water coolant temperature near or at saturation. Most of the tests resulted in spontaneous explosions with conversion ratios in the lower end of the observed range (0.2 to 0.3%). This behavior is in contrast to the small-scale experiments where explosions with high-temperature water could only be induced by using a larger artificial trigger. This suggests that the effect of coolant temperature may be scale dependent. Previous models[11] for molten metal-water

[8]The conversion ratio is defined as the ratio of the experimental work measured to the fuel thermal energy.

[9]A thermitically generated melt is one in which an exothermic oxidation-reduced chemical reaction is used to produce, for example, molten iron and alumina from iron-oxide and aluminum.

[10]Corium-A+R stands for a fuel melt with a large quantity of stainless steel added to simulate some portion of the melted reactor vessel: stainless steel = 59%, UO_2 = 23%, ZrO_2 = 15%, and NiO = 3% (at.%).

[11]M. L. CORRADINI, W. M. ROHSENOW, and N. E. TODREAS, "A Proposed Model for Tin-Water Interactions," *Proc. Mtg. Two-Phase Heat Transfer and Flow*, American Society of Mechanical Engineers, San Francisco, California, December 1978.

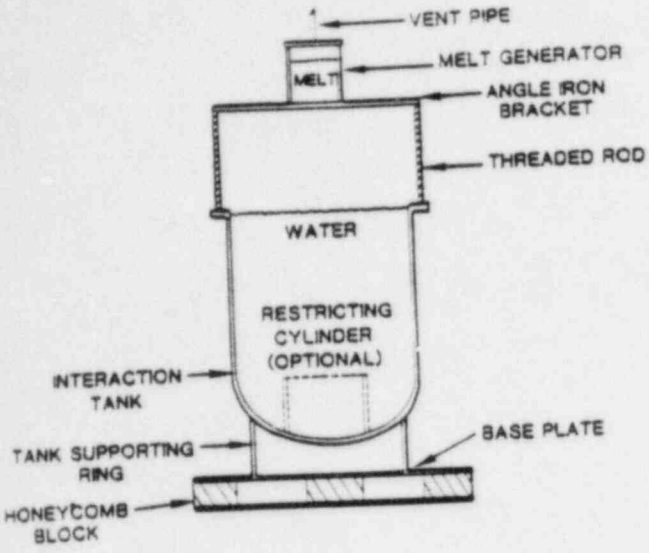

Fig. 1. Interaction vessel as used in open geometry experiments.

TABLE I

Open Geometry Experimental Observations (Refs. 4 and 5)

Conversion ratio	
	The explosion conversion ratio with Fe-Al_2O_3 was between 0.2 and 1.4%.
	Water temperature had little effect on the conversion ratio.
	No energetic explosions with Corium-A+R were observed; a maximum conversion ratio was <0.05% using a large detonating cord trigger (~6 g PETN explosive).
Parametric effects	
	No obvious pour rate effect
	No interaction volume effect
	Possible melt quantity effect
	Definite water quantity effect; as the mass of water increased, the conversion ratio increased.
Pressures	
	High narrow pressure spikes possible (20 MPa, <1 ms) 5- to 10-MPa sustained pressures in large explosions
Triggering	
	Spontaneous explosions were observed only for the Fe-Al_2O_3 melt and seemed to involve solid surface contact.
	Artificial triggers (0.6 g PETN explosive) were used for the Fe-Al_2O_3 melt, but did not modify the conversion ratio.
	Only when the trigger magnitude was substantially increased did a small explosion occur with Corium-A+R.
Debris	
	Debris was similar to that observed in small-scale arc-melter experiments for the Fe-Al_2O_3 fuel melt.

simulant systems have proposed this. The film collapse model used to specifically analyze the small-scale experiments does not directly predict this.[7,12] The implication for reactor safety application based on these test results is that the initial coolant temperature is not a sufficient barrier to preclude an energetic explosion.

II.A.2. Fuel Composition–Noncondensable Gases

In most of the 50 large-scale tests, the Fe-Al_2O_3 fuel melt exploded vigorously. In small-scale experiments, stainless steel or iron did not explode; subsequently, Nelson et al.[3] suggested that noncondensable gas (H_2), generated from oxidation of the metallic phase of the fuel melt by steam, could suppress the explosion. Analysis of the Nelson tests[7] indicated that the noncondensable gas acted as a cushion, stabilizing the film against collapse from an external trigger. This difference between large and small scale suggests that the effect of noncondensable gases may also be scale dependent.[13]

The rate of noncondensable gas formation can be scale dependent. Because it is based on the surface area exposed to steam, as the volume increases, the surface-to-volume ratio decreases, and thus, the gas volume surrounding the fuel would decrease. Therefore, the gas film might not be as stable, and instability effects could trigger the explosion, e.g., an external pressure perturbation, solid surface contact, or random boiling processes on a more planar surface.

Another important consideration in the large-scale experiments is that there is a molten oxide phase, Al_2O_3, that could be exploding first and, subsequently, triggering the metallic iron phase.

[12]M. L. CORRADINI, "Analysis and Modelling of Steam Explosion Experiments," SAND80-2131, Sandia National Laboratories, to be published in 1981.

[13]Molten steel explosions in foundry accidents are another example of large-scale interactions.

Aluminum oxide is a relatively low-melting-point oxide ($T_m \sim 2300$ K) compared to the prototypic reactor oxides (for uranium-zirconium-oxygen, $T_m \sim 2800$ K), and the initial temperature of the Fe-Al_2O_3 melt is high, ~2800 K; therefore, the oxide phase is molten and substantially above its melting temperature. The Al_2O_3 could be the fuel melt component to first undergo an interaction, and the pressure pulse generated by fuel fragmentation and steam formation could then collapse the gas-vapor film surrounding the iron. Nelson[6] has successfully generated explosions using molten Al_2O_3 and water, so it is not inconceivable that this process occurs at a large scale.

II.A.3. Fuel Composition–Solidification

When the fuel composition was changed to Corium-A+R, the explosion conversion ratio decreased significantly; in fact, in all four of the experiments performed, no spontaneous energetic explosions like those using Fe-Al_2O_3 were observed. The largest conversion ratio from a triggered explosion was ~0.05%, which is smaller than the energy of the trigger needed. In past analyses,[7,14-18] it has been proposed that the oxide phase of the fuel could solidify and that this retarding effect, coupled with noncondensable gases suppressing a metallic phase interaction, explained the lack of explosivity. This same explanation is valid for Corium-A+R, because the only difference is that the mole fraction of stainless steel has increased.

Solidification of the oxide phase of Corium-A+R could explain the lack of explosivity. The oxide (uranium-zirconium-oxygen) has a liquidus temperature of ~2800 K in comparison to a melting temperature of 2300 K for Al_2O_3. For both fuel melts, the initial temperature of the melt before it was delivered to the water was ~2800 K; therefore, the Corium oxide phase was probably at or below its liquidus temperature. A simple cooling analysis was done to indicate that the melt could have cooled substantially in its fall through the air and water before an external trigger was fired to induce an interaction.[6,12]

In the Buxton and Benedick Corium tests, the explosion was nonenergetic even when the trigger was substantially increased in size. No spontaneous explosion occurred, and no explosions occurred when a detonator trigger was used (0.6 g of PETN explosive; energy = 0.36 kJ). Only when a primacord explosive trigger was used (6 g of PETN explosive; energy = 3.60 kJ) did a minor interaction occur (conversion ratio = 0.05%; work = 3.0 kJ). If the solidification of the oxide phase is the cause of this behavior, it suggests that it is somewhat trigger dependent although the explosive yield is very small even when a very large trigger is used.

III. FULLY INSTRUMENTED TEST SERIES

Within the last year, the second large-scale experimental series has begun, designated FITS. The purpose of these tests is to determine the explosion conversion ratio as a function of ambient pressure, fuel composition, and other initial conditions in an enclosed interaction chamber (Fig. 2). The experiments are instrumented to provide measurements of short- and long-term pressure data, work, fuel debris characterization, and visual observation of the explosion. Up to the present time, Mitchell has performed 20 preparatory experiments outside the chamber EXO-FITS and 5 in-chamber experiments. These initial checkout tests have used ~5 kg of Fe-Al_2O_3 fuel simulant injected into water. Preliminary results from these experiments are given in Table II. The key observations to date[6] are as follows:

1. The large-scale interaction visually resembles a detonation-like structure seen in chemical explosions.[19,20]
2. The peak pressures are large, but decrease quite quickly to sustained pressures similar to Buxton's reported values.[4]
3. A violent explosion can be triggered at a high-ambient pressure (1.0 MPa) by increasing the trigger size.

[14]D. A. POWERS, *Core Meltdown Experimental Review*, Chap. 4, SAND74-0394, Sandia National Laboratories (1975).

[15]A. GANGULI and S. G. BANKOFF, "Mechanics of Vapor Explosions," *Third CSNI Specialists' Mtg. Sodium-Fuel Interactions in Nuclear Reactor Safety*, Tokyo, Japan, March 1976.

[16]A. SHARON and S. G. BANKOFF, "Propagation of Shock Waves Through a Fuel-Coolant Mixture; Part B: Taylor Instability," COO-2512-14, Northwestern University (May 1978).

[17]S. G. BANKOFF, "Vapor Explosions: A Critical Review," *Proc. 6th Int. Heat Transfer Conf.*, Toronto, Canada, August 7-10, 1978, CONF-780807.

[18]L. D. BUXTON, "Molten-Core/Water Contact Analysis for Fuel Melt Accidents," SAND77-1842, NUREG/CR-0391, Sandia National Laboratories (Feb. 1979).

[19]S. L. THOMPSON, "CSQ-II, An Eulerian Finite Difference Program for Two-Dimensional Material Response," SAND77-1339, Sandia National Laboratories (Feb. 1979).

[20]M. L. CORRADINI, R. L. WOODFIN, and L. E. VOELKER, "Preliminary Analysis of the Containment Failure Probability by Steam Explosions Following a Hypothetical Core Meltdown in a LWR," SAND79-2002, NUREG/CR-1104, Sandia National Laboratories (Feb. 1980).

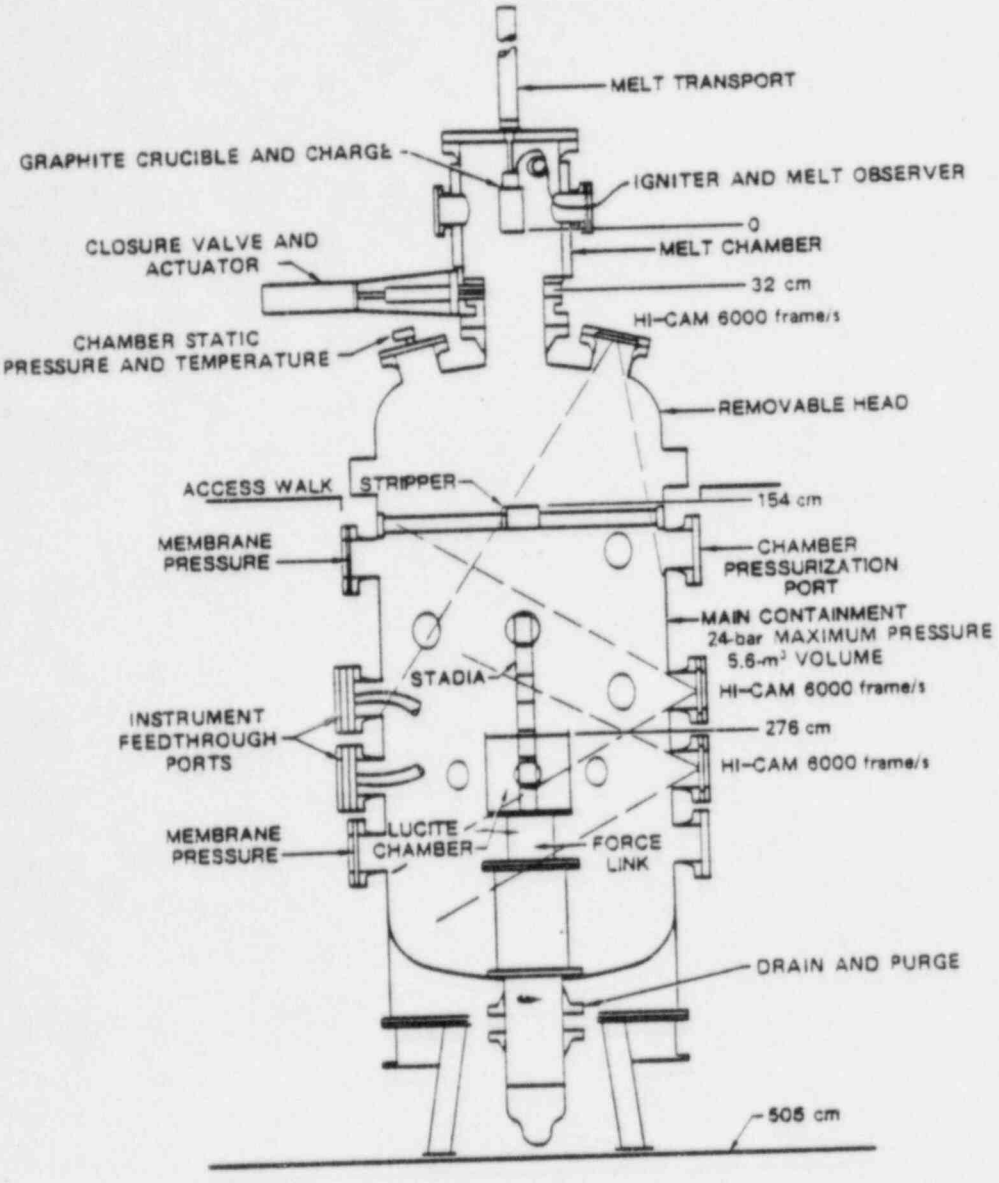

Fig. 2. FITSA series experimental apparatus.

III.A. Effect of Fuel Mass and Entry Velocity

In the initial experiments performed outside the chamber, it was found that spontaneous explosions could be generated only if the fuel mass was above certain limits ($m_f \geq 2$ kg) and the entry velocity was below certain limits ($U = 6$ to 8 m/s). The reason for these empirical thresholds is not clear.

One possible reason may be that these large-scale experiments are affected by entrained noncondensable air in the same way as the single droplet experiments of Nelson et al.[3] Nelson et al. noted that spontaneous interactions were suppressed if the fuel fall height was increased (i.e., the entry velocity was increased). They visually observed more entrained air as the velocity increased. Similarly, Mitchell delivered the fuel into the water in the form of a single molten mass, similar to a large droplet (the molten mass began to deform due to hydrodynamic forces before it entered the water, but visual observations still indicate that it did not fragment). Noncondensable gas may also be the explanation for the explosion suppression.

The effect of the fuel mass on spontaneity can also be attributed to noncondensable gas. May,[21] in his water entry experiments using a steel ball, found that not only does the ratio of entrained gas volume to the steel ball volume decrease as the velocity (fall height) decreases, but also as the steel mass

[21] A. MAY, "Dependence of the Water-Entry Cavity on the Surface Condition of a Missile Model," NAVORD Report 1963 U.S. Naval Ordinance Test Station, China Lake, California (Jan. 1951).

TABLE II

FITS Experimental Observations

Conversion ratio	
	The explosion conversion ratio with Fe-Al_2O_3 is consistently near 2 to 3%.
Pressures	
	High narrow pressure spikes are always observed (~20 MPa for ~1 ms).
	Lower sustained pressures follow behind this peak.
Propagation behavior	
	The fuel coarsely intermixes with the coolant prior to the interaction (time ~0.2 s).
	A spontaneous explosion begins near the chamber base.
	A detonation-like explosion wave is observed.
	The explosion velocity varies between 200 and 600 m/s.
Initial conditions	
	As the fuel entry velocity is increased (>6 m/s) or the fuel mass decreased (≤2 kg), spontaneous explosions are suppressed.
Debris	
	The weight-averaged mean particle size after the explosion is ~150 to 250 μm, and without an explosion ~1 to 3 mm.
High-ambient pressure	
	A violent explosion was produced at an ambient pressure of 1.1 MPa by using an artificial trigger. The trigger was a detonator like that used in the open geometry tests (0.6 g of PETN explosive).

increases. This same effect was also predicted for simulant fuel-coolant systems.[11] This same effect could be occurring here: the fuel mass increases, and less noncondensables are entrained around the fuel thereby allowing a spontaneous interaction to occur.

IV. A TRANSIENT ONE-DIMENSIONAL EXPLOSION PROPAGATION MODEL

In Mitchell's experiments,[6] once the explosion is triggered, it is observed to propagate through the fuel-coolant mixture; after a time this propagation is almost one-dimensional in nature. High-peak pressures (20 MPa) are measured at the leading edge of the explosion wave as it propagates quickly (200 to 600 m/s) through the mixture. Physically, the propagation phase of the steam explosion is composed of a series of vapor film collapses (Fig. 3), similar in concept to what occurs in the Nelson et al. single droplet tests.[3] Each film collapse causes the enclosed drop to fragment and transfer its thermal energy to some of the surrounding coolant via rapid steam production. This increase in vapor production results in elevated pressures in the coolant region surrounding the droplets and stimulates an even more rapid collapse of the neighboring vapor films.

The analogy to a line of dominoes is appropriate to this phase of the interaction. The system is stable as long as one of the dominoes is not pushed into its neighbor. However, once one of them is pushed over, i.e., triggered, the chain reaction begins and propagates as if each succeeding domino were larger than the last.

A multiphase one-dimensional transient model was developed to describe this propagation phenomenon. The model includes three materials—fuel droplets, vapor, and liquid coolant. A number of assumptions are employed in the analysis:

1. The multiphase flow regime used in the model is assumed to be fuel droplets surrounded by a vapor film in a continuous medium of liquid coolant.
2. The fuel-coolant mixture is assumed to be homogeneous, i.e., one single droplet diameter, film thickness, and droplet spacing characterize the fuel-coolant mixture.
3. Relative bulk velocity between the fuel and the coolant is neglected.
4. Vapor film collapse and the subsequent vapor expansion are assumed to be spherically symmetric.
5. Constant thermophysical properties are assumed for the fuel and coolant.
6. The vapor is assumed to behave as a perfect gas.

The first two assumptions are important with respect to the macroscopic behavior of the explosion. In the FITS experiments, the fuel drops into the coolant as an essentially unfragmented mass and then begins to mix with coolant in a film boiling mode (Fig. 4). It breaks up into smaller droplets as the water interpenetrates, and a fuel-coolant mixture is formed. To assume that the fuel-coolant mixture is a series of separate droplets with a vapor film in water all with some characteristic dimensions is a gross simplification. What the actual system mixture looks like is unknown. One possible picture is shown in Fig. 5. Fuel-coolant mixing is actually

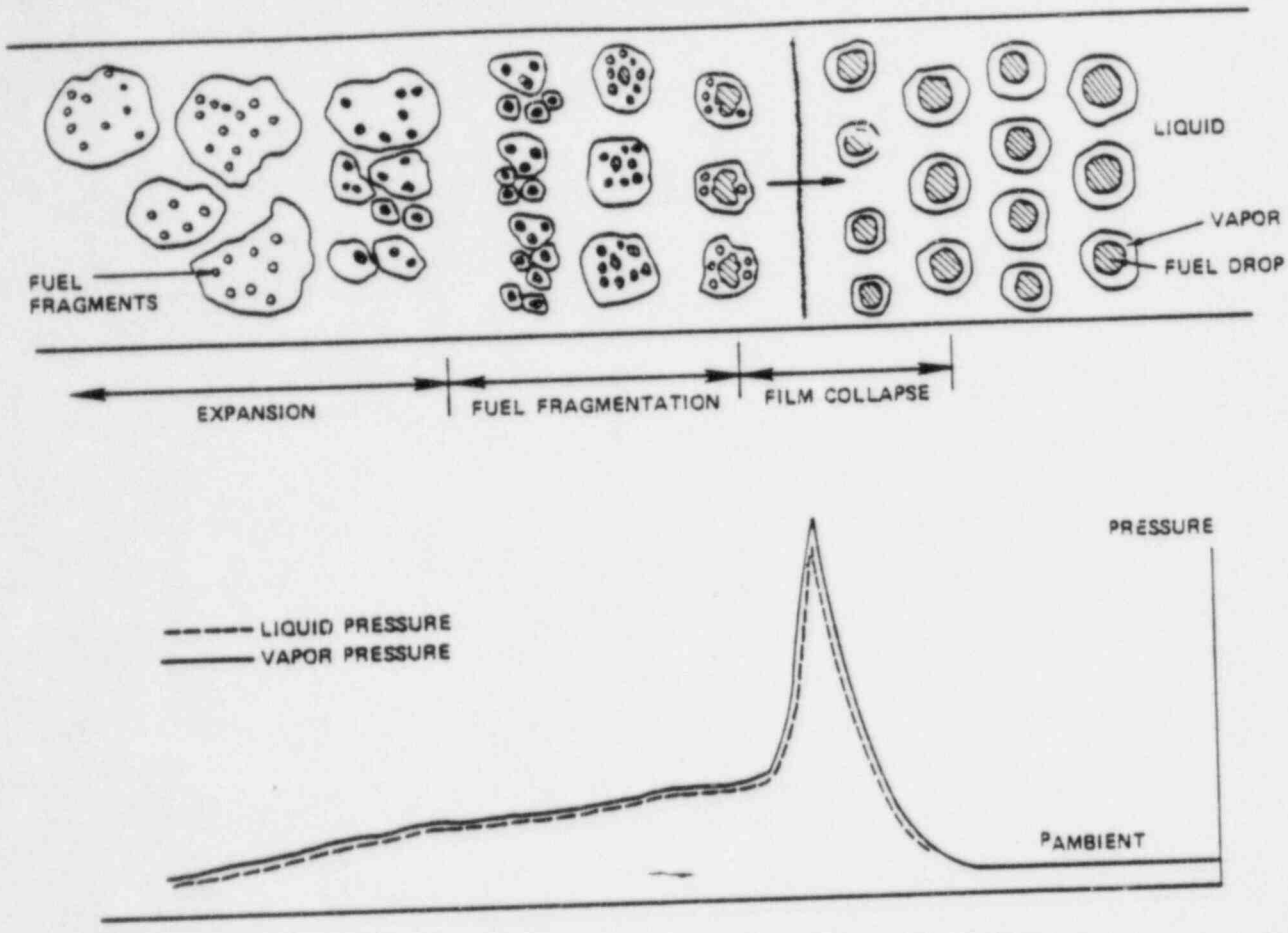

Fig. 3. Steam explosion propagation zone in a large fuel-coolant mixture.

occurring at the outer edges of the real multidimensional system. As the water penetrates inward, the outer edges of the fuel-coolant mixing zone are probably well represented by the first assumption. However, as one moves closer to the center, the vapor volume fraction probably increases significantly as steam bubbles (and probably hydrogen bubbles from iron oxidation) agglomerate. In addition, there would be a spectrum of fuel droplet diameters and relative spacing, rather than one set of representative values. Therefore, in employing the first two assumptions, it is recognized that the one-dimensional model is only a first approximation of the real system. Future work will attempt to remove some of these simplifications.

The third assumption is known to be in error for the initial stages after film collapse, when the coolant bulk velocity would be larger than the fuel. However, velocity equilibration occurs quite quickly and, therefore, the assumption should be viewed as a reasonable first approximation. To accommodate fuel fragmentation due to fuel-coolant relative velocities, this assumption can be relaxed to some extent to compute the fuel droplet breakup time.

The assumption of spherical symmetry during film collapse and subsequent steam expansion after the explosion is believed to be reasonable as a first approximation. Asymmetric effects may become important only in the final stages of film collapse, and the fuel fragmentation model used in this analysis considers this.

The remaining two assumptions are reasonable for this one-dimensional model. More detailed equations of state for the liquid and the vapor could be included, but this seems to be unwarranted at this time, given the uncertainty in the physical mechanisms.

A key ingredient in the model is the mechanism for fuel fragmentation that initiates and sustains the explosion. At the present time, two fragmentation mechanisms are considered possible; these mechanisms can separately or jointly cause the rapid fuel fragmentation observed, and significantly increase the heat transfer rate during the final stages of film collapse. The first model, a thermal mechanism, assumes that high vapor pressures due to rapid steam generation after film collapse cause Taylor instabilities that fragment the fuel. This mechanism was used to successfully model the single droplet experiments of Nelson.[12] The second model,

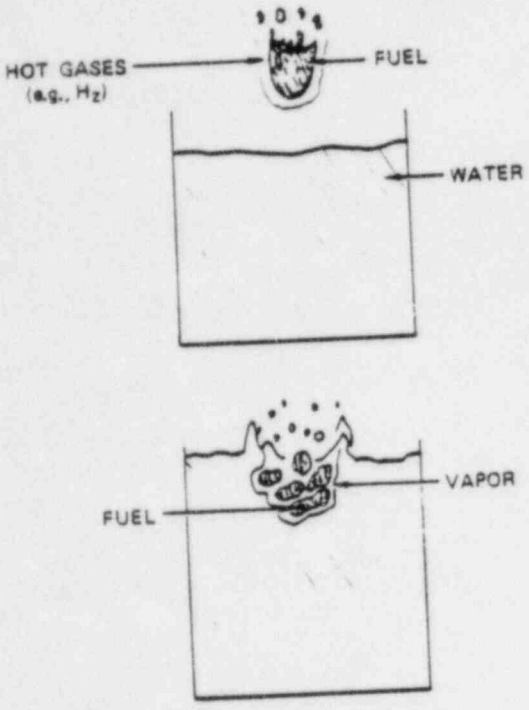

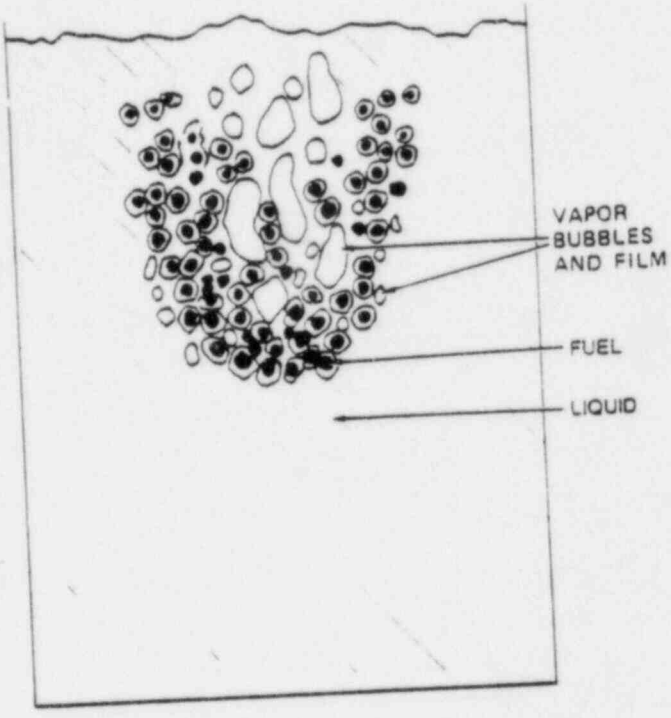

Fig. 5. Possible fuel-coolant mixture geometry.

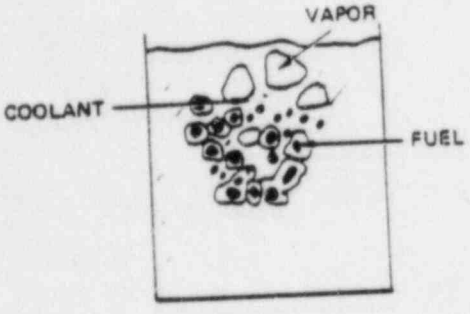

Fig. 4. FITS initial fuel-coolant mixing.

a mechanical mechanism, assumes that the impact of the coolant liquid upon the fuel droplet during film collapse causes cavitation and subsequent fragmentation of the fuel. This model was originally used by Drumheller[22] in parametric calculations to demonstrate its feasibility.

The one-dimensional Lagrangian hydrodynamic wave code, WONDY-IV (Ref. 23), was modified to incorporate this multiphase system and these two fragmentation models. This wave code was designed to solve conventional continuum relations, but was easily modified for this problem. In WONDY the explicit finite difference algorithm solves the mass and momentum equations simultaneously for new values of density, $\rho(t^{n+1})$, position, $x(t^{n+1})$, and velocity, $v(t^{n+1})$, using old values of pressure, $P(t^n)$, and internal energy, $E(t^n)$. Then the equations of state and conservation of energy are solved simultaneously for $P(t^{n+1})$ and $E(t^{n+1})$. The mass and momentum formulations already contained in WONDY are sufficiently general and can be used without modification for this multiphase system of fuel, vapor, and liquid coolant. For example, the mass equation is[24]

$$\frac{d}{dt}(\rho_m x) = 0 \quad . \tag{1}$$

where x is the position.

The quantity ρ_m is the mixture density given by

$$\rho_m = \rho_f \alpha_f + \rho_v \alpha_v + \rho_c \alpha_c \quad , \tag{2}$$

where $\alpha_{f,v,c}$ are the volume fractions of the fuel, vapor, and liquid coolant, respectively, subject to the constraint

$$\alpha_f + \alpha_v + \alpha_c = 1 \quad . \tag{3}$$

Only the equations of state and energy for the fuel, vapor, and liquid need to be rewritten and included in the WONDY formulation. These field equations in a multiphase formulation are

[22]D. S. DRUMHELLER, *Nucl. Sci. Eng.*, **72**, 347 (1979).

[23]R. J. LAWRENCE and D. S. MASON, "WONDY-IV, A Computer Program for One-Dimensional Wave Propagation with Rezoning," SC-RR-710284, Sandia National Laboratories (1975).

[24]A Nomenclature appears on p. 446.

local statements for one particular numerical mesh cell; i.e., they do not contain spatial gradients from neighboring mesh cells, and thus are solved separately in a subroutine. Therefore, only this subroutine was reformulated.

This subroutine is constructed in the following manner. First, the old and new values of density, ρ_m, are linearly interpolated to give a continuous value of ρ_m across a time step, $t^{n+1} - t^n$. Then the energy equations, equations of state for the fuel and coolant, and the vapor-film collapse relation (Rayleigh momentum equation) are viewed as a system of nonlinear ordinary differential equations in time. Finally, these equations are integrated from the old value of time across the time step to the new value of time using a Runge-Kutta numerical technique. This method provides the new value of mixture energy and pressure that is required by the mixture mass and momentum equation for continued computation. A more detailed description of the governing equations is given in the Appendix.

This one-dimensional model was used to investigate the effect of initial conditions on the propagation of a large-scale explosion, as observed in the FITS experiments. A one-dimensional 0.75-m-long channel was chosen as the base case with 25-mm-thick numerical mesh cells. Each mesh cell contains a fuel droplet (D_f = 20-mm diam) surrounded by a vapor film (δ_v = 0.6 mm thick). These characteristic dimensions give values that are in the range of the FITS conditions and agree qualitatively with visual observations. Figure 6 illustrates this base case calculation wave profiles at different times after trigger pulse application. The trigger was assumed to be 10.0 MPa for 50 μs. This value corresponds to what would be expected if water were to undergo homogeneous nucleation if it is entrapped by the fuel melt. This mechanism was considered to be a plausible cause of the spontaneous trigger. Because local film collapse and steam bubble expansion are calculated, the pressure and the temperature within the vapor and liquid are not the same (even though the pressures far exceed the critical pressure of 22.1 MPa); therefore, both liquid and vapor pressures are plotted. At the head of the left-traveling wave is a growing pressure peak, which is a result of film collapse and initial fuel fragmentation without significant steam expansion. By 0.6 ms, a pressure wave was attained (135 MPa), which is above the upper range of Mitchell's data.[6] The explosion wave velocity is ~900 m/s, which is larger than what Mitchell observed.[6] In these calculations, the thermal fuel fragmentation mechanism was employed. The vaporization of the coolant is shown by the sustained lower pressures behind the explosion wave. The pressure decrease with distance from the peak at a fixed time indicates that the vapor expansion phase has begun.

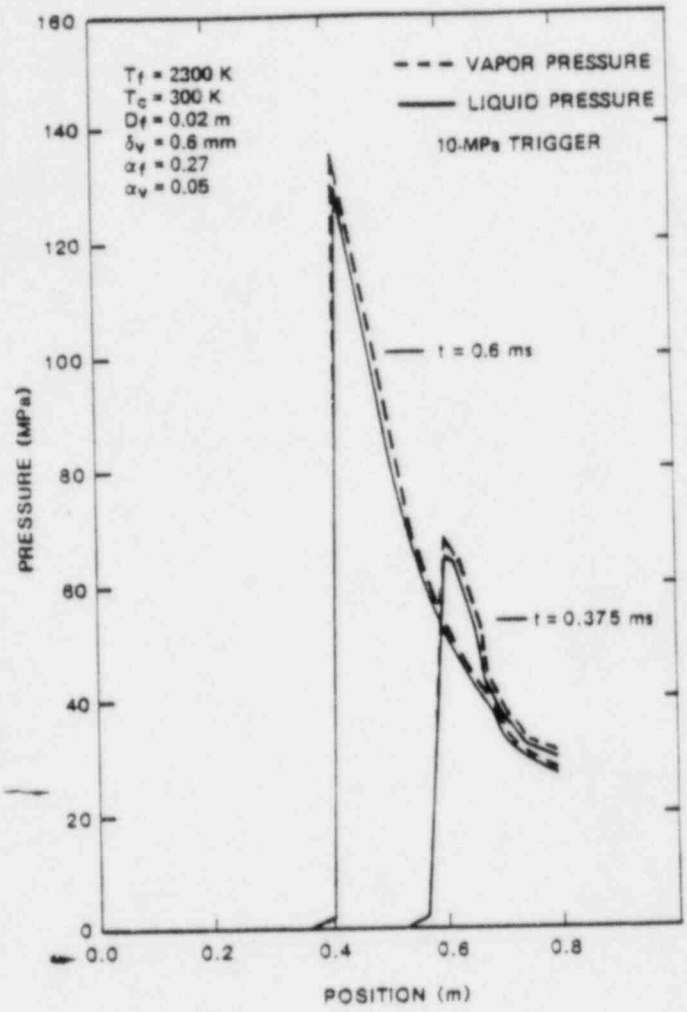

Fig. 6. One-dimensional calculation using the thermal fuel fragmentation mechanism (α_f = 0.27).

A parametric study was done to investigate the effect of the trigger magnitude, and the vapor and fuel volume fraction, on the explosion behavior over a range of values observed in FITS. The initial conditions are given in Table III along with the resultant explosion wave velocity. Note that the propagation velocity decreases significantly as the film thickness, α_v, and, therefore, δ_v increases. This is also illustrated in Fig. 7 and Table III for cases 1 and 4. Also, the figure indicates that the peak explosion pressure decreases as the vapor volume fraction increases. Both of these results are caused by the vapor adding more compressibility to the fuel-coolant system. Therefore, as the film collapses, more vapor still remains in the mixture, and this slows the transmission of the pressure wave to neighboring films and lowers the peak pressure in the region of the explosion. If the trigger pressure is reduced, the propagation velocity also decreases (Table III); if the trigger is decreased sufficiently, the explosion does not propagate at all. The reason

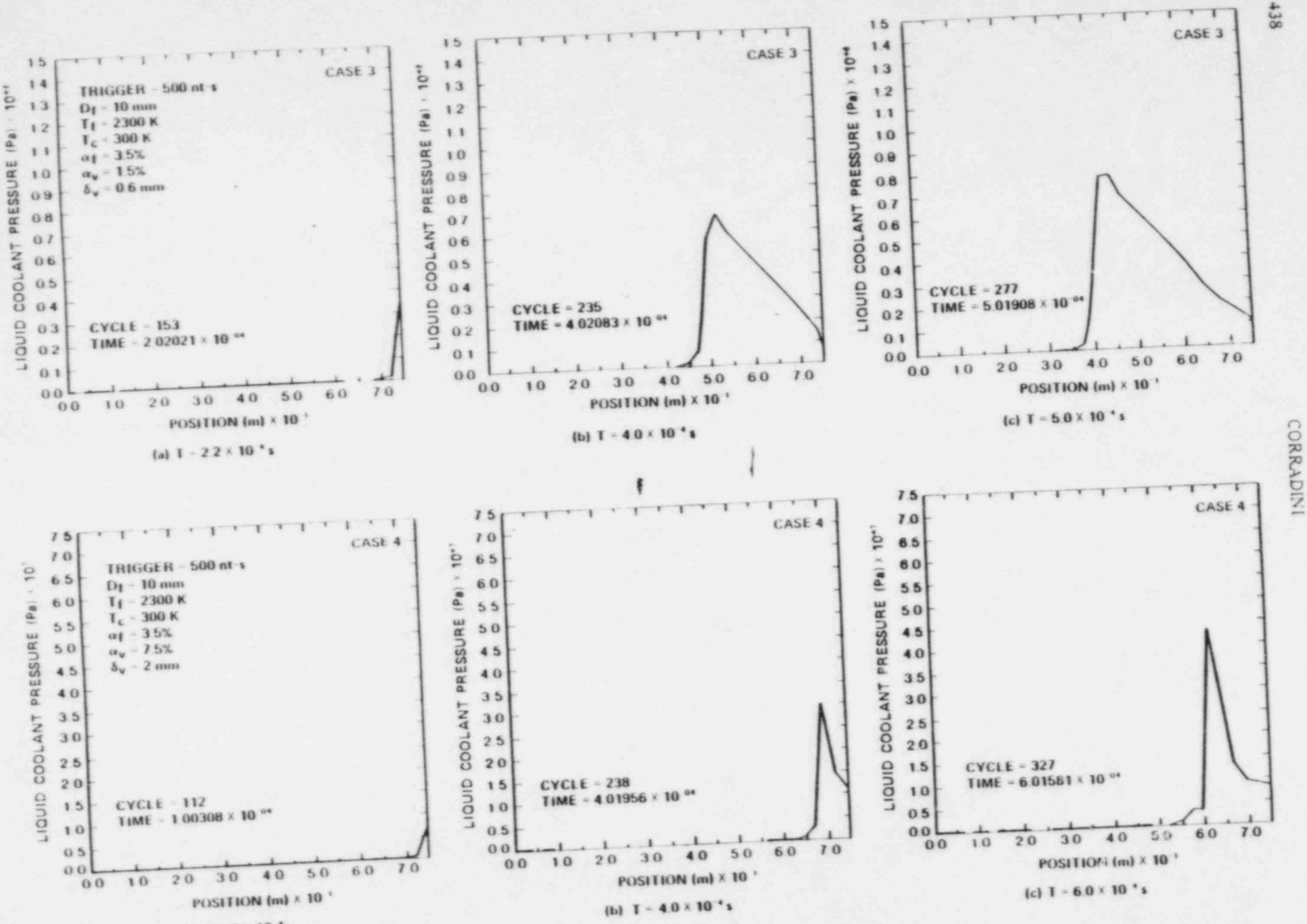

Fig. 7 One-dimensional calculation using the thermal fuel fragmentation mechanism cases 3 and 4.

TABLE III

Summary of Initial Conditions Effects on the Explosion Propagation Velocity

Case Number	Trigger Magnitude, $P_p - P_\infty$ (MPa)	Fuel Drop[a] Diameter, D_F (m)	Initial Steam Film Thickness, δ_v (mm)	Initial Fuel Volume Fraction,[b] α_f	Initial Steam Volume Fraction,[c] α_v	Explosion Propagation Velocity, V_D (m/s)
1	10	0.01	0.6	0.035	0.015	750
2	3	0.01	0.6	0.035	0.015	500
3	1	0.01	0.6	0.035	0.015	No propagation
4	10	0.01	2	0.035	0.08	350
5	10	0.01	6	0.035	0.45	100

[a]Initial fuel temperature (T_F) = 2300 K; initial coolant temperature (T_c) = 300 K; and thermal fuel fragmentation mechanism.

[b]$\alpha_f \equiv \dfrac{\frac{\pi}{6} D_F^3}{\text{unit cell volume}}$.

[c]$\alpha_v \equiv \dfrac{\frac{\pi}{6}(D_F + \delta_v)^3 - D_F^3}{\text{unit cell volume}}$.

for this behavior is that the film collapse process is slowed. As the trigger weakens, the film does not collapse as completely; consequently, local pressures generated by droplet fragmentation are reduced and subsequent film collapses are slowed: the whole propagation process is retarded.

The final important observation that we made from these calculations is that the explosion propagation escalates in pressure slowly, and the calculation never indicated a steady-state detonation, for example, as has been assumed by Board et al.[25,26] This has two important implications. Practically, the explosion mixture dimensions will probably not be larger than 1 or 2 m, and therefore, we would not observe a steady-state detonation for these initial conditions. Therefore, using explosion work estimates based on this assumption is conservative in some cases. Second, from a theoretical viewpoint, if the explosion escalates very slowly, then the role of hydrodynamic fragmentation due to induced relative velocities may be irrelevant. In previous work, Corradini[7,12] has shown that purely hydrodynamic fragmentation due to relative velocities cannot explain Nelson's single droplet fuel fragmentation,[6] and, therefore, cannot be used to explain the escalation of the explosion for large-scale tests. If indeed the escalation phase dominates the real explosion process, then relative velocity-induced hydrodynamic fragmentation is neither a necessary nor a sufficient condition to sustain the explosion.

V. AN EMPIRICAL TWO-DIMENSIONAL EXPLOSION MODEL

In the FITS experiments, the explosion exhibits multidimensional characteristics. These characteristics could cause a nonuniform pressure loading of the surrounding structure and can mitigate the explosive work potential from what would be predicted by a one-dimensional analysis. This same situation also exists in the full-scale reactor situation. Because of this, a simple empirical explosion model was developed and incorporated into the two-dimensional hydrodynamics CSQ code.[19]

The steam explosion is modeled as a chemical explosion. The empirical explosion model considers the water and the steam intermixed with the melt to be analogous to a chemical explosive (M_{EXP}) and considers the thermal energy of the melt to be analogous to the chemical heat of reaction released to the coolant during the explosion (Q_{EXP}). This model is based on the concept that the fuel melt and the coolant in the explosion zone interact and come to thermal equilibrium before substantial coolant expansion occurs. This can be expressed mathematically by an energy balance neglecting the coolant expansion:

[25]S. J. BOARD et al., *Nature*, **254**, 319 (1975).

[26]S. J. BOARD et al., "Recent Advances in Understanding Large Scale Vapor Explosions," *Third Specialists' Mtg. Sodium-Fuel Interactions in Fast Reactors*, Tokyo, Japan, March 1976, CONF-760328.

$$(m_c u_c + m_v u_v + m_f u_f)_i = (m_c u_c + m_v u_v + m_f u_f)_e \quad (4)$$

where

$$u_c = c_{v_c} T_c \quad (5)$$

$$u_v = c_{v_v} T_v \quad (6)$$

$$u_f = c_{v_f} T_f \quad (7)$$

i = initial temperature

e = equilibrium temperature.

The equilibrium temperature can be found by solving

$$T_e = \frac{m_c c_{v_c} T_c + m_f c_{v_f} T_f + m_v c_{v_v} T_{v_i}}{m_c c_{v_c} + m_v c_{v_v} + m_f c_{v_f}} \quad (8)$$

This equilibrium temperature can be used to determine the analogous heat of reaction (Q_{EXP}) released to the coolant (M_{EXP}) as if a chemical explosion occurred. This is given by

$$Q_{EXP} = m_f c_{v_f} (T_{f_i} - T_e) \quad (9)$$

$$M_{EXP} = m_c + m_v \quad (10)$$

This energy is then deposited into the water and steam in the explosion zone, and using an analytic equation of state for the coolant, the resultant temperature and pressure in the region are calculated.

This explosion model was incorporated into CSQ. The water and steam are initially input as a two-phase mixture in the region of the explosion zone. Then the calculation is started with the explosion being triggered in a one-mesh cell. The fuel melt thermal energy is then deposited into the two-phase mixture, and the code calculates the pressure-wave/particle-velocity effects in the surrounding liquid and structure. Two different equations of state for the water involved in the explosion can be used in CSQ:

1. a general analytic equation of state without any restrictions on coolant pressure or temperature
2. the analytic equation of state for water (steam tables) with a peak pressure restriction of 300 MPa.

In the present calculations, the more accurate steam table equation of state was used.

The mass of coolant involved in the explosion is the only parameter in the model. This value is adjusted so that the calculation causes an explosive steam production rate that results in pressure-time behavior and coolant kinetic energy, which agrees with that observed in the FITS experiments. In this way, the ratio of the mass of fuel melt and coolant, which participate in an explosion for any given experiment, can be empirically determined. This ratio is important because it is the major unknown quantity in previous experiments.

The local thermal equilibrium approach is, we believe, approximately valid for analyzing macroscopic effects because the explosion propagation velocity is quite large (200 to 600 m/s) and, therefore, the explosion propagates spatially before any significant expansion occurs. It is also felt this model can give some insight into the experiments in terms of explosion propagation velocity and mass of coolant participating for a given mass of fuel.

A simple calculation is shown in Figs. 8, 9, and 10 for representative conditoins of the FITS experiments:

m_f = 5 kg

T_f = 2300 K

α_v = 0.35

T_c = 300 K

The mass of coolant assumed to participate in the explosion is 10 kg with a detonation velocity of 300 m/s. This corresponds to a Q_{EXP} of 1.2 MJ/kg of coolant. The dot density plots of pressure indicate that the explosion produces peak pressure pulses of the order of 100 MPa, lasting for times of ~200 μs and then falling to much lower values. These pressure-time results are in good agreement with FITS data (Fig. 10), suggesting that the assumed mass ratio may be near that amount that participated in the actual explosion.

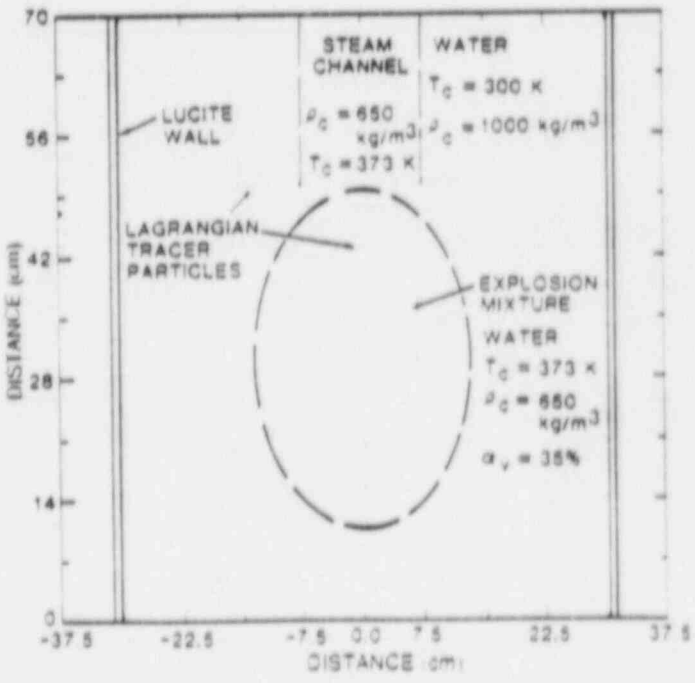

Fig. 8 Initial geometry and conditions for calculation of FITS test MD-19.

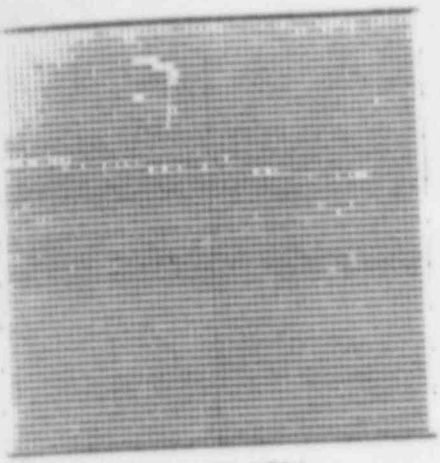

(a) SPACE MESH

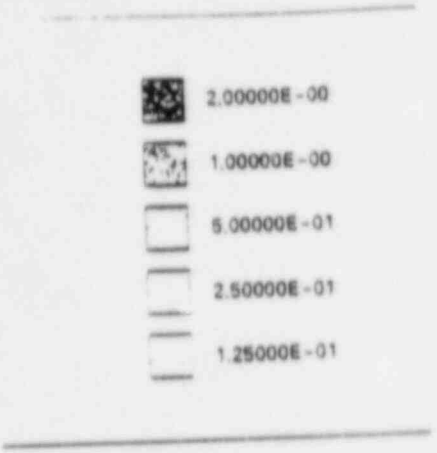

(b) DENSITY SCALE (g/cm³)

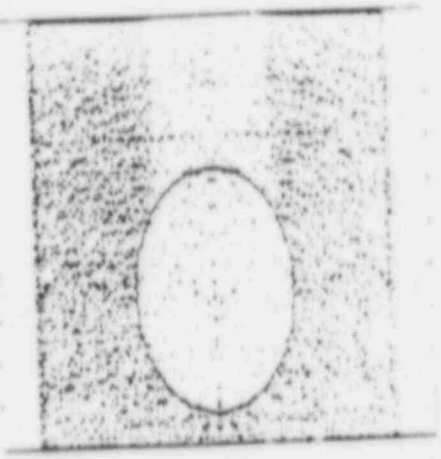

(c) t = 0.2 ms

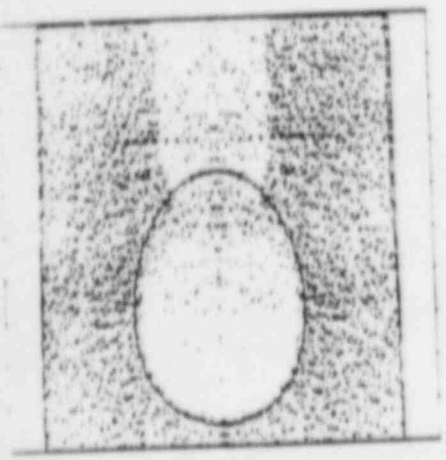

(d) t = 1.0 ms

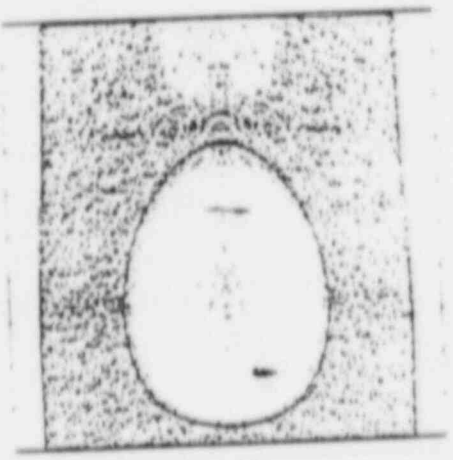

(e) t = 1.4 ms

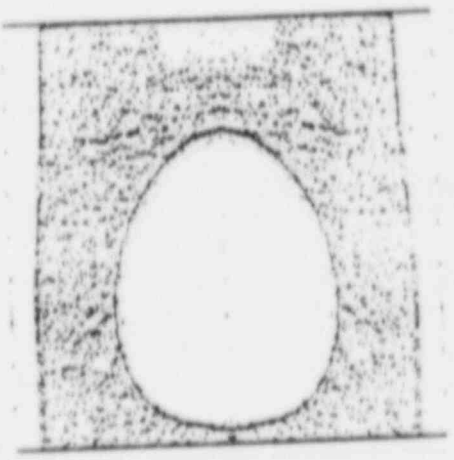

(f) t = 1.6 ms

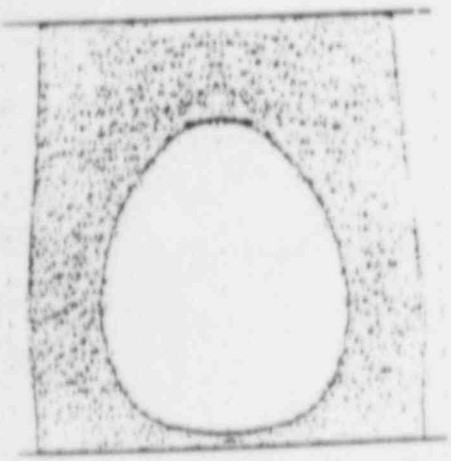

(g) t = 1.8 ms

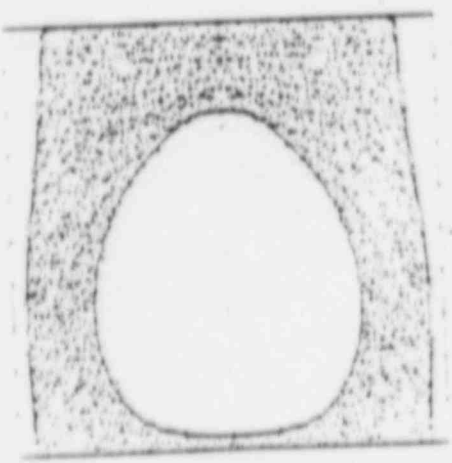

(h) t = 2.0 ms

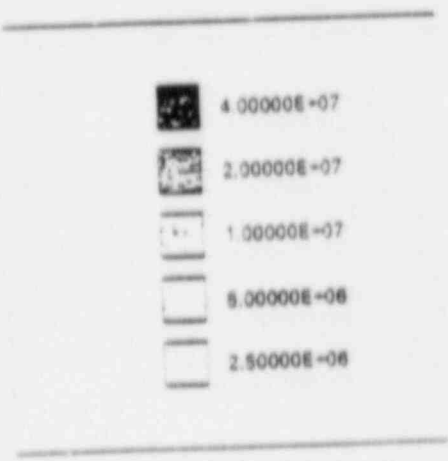

(i) PRESSURE SCALE (dyne/cm²)

Figs. 9a through 9i. Dot density plots of material density and pressure for CSQ calculation.

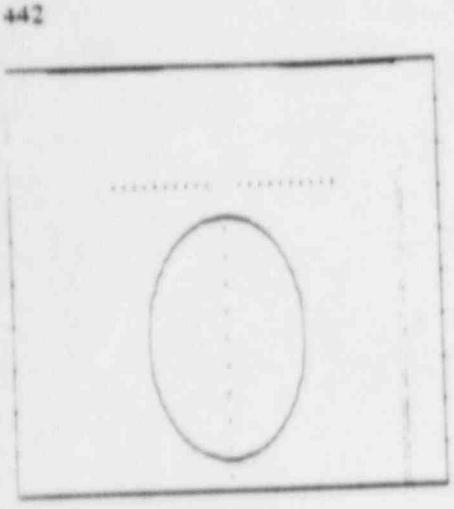

(j) t = 0.0

(k) t = 0.2 ms

(l) t = 0.4 ms

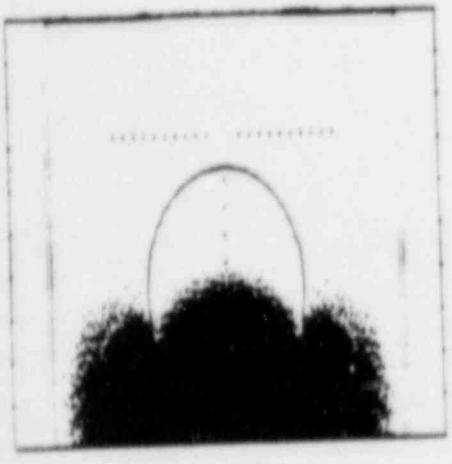

(m) t = 0.6 ms

(n) t = 0.8 ms

(o) t = 1.0 ms

(p) t = 1.2 ms

(q) t = 1.4 ms

(r) t = 1.6 ms

Figs. 9j through 9r. Dot density plots of material density and pressure for CSQ calculation.

(s) t = 1.8 ms (t) t = 2.0 ms

Figs. 9s and 9t. Dot density plots of material density and pressure for CSQ calculation.

Note that in the FITS experiments, the actual mass of coolant in the explosion zone was observed to be much greater than 10 kg. The fuel actually dispersed into the coolant to an extent corresponding to ~20 to 40 kg of coolant in the explosion zone. But not all of this coolant participated in the initial explosion interaction. If it did, the predicted steam pressures would be initially much lower (1.0 to 2.0 MPa) than what is observed. Therefore, most of the coolant in the explosion zone does not participate in the explosion initially. This is in agreement with the one-dimensional explosion model where most of the coolant surrounding the fuel is not vaporized. However, after the fuel has equilibrated, it is possible that additional coolant does participate during the expansion phase due to entrainment and convective mixing further cooling down the high-pressure steam. It can further reduce the explosion work potential by a factor of 2 or more. This empirical model is now being used for analysis of FITS experiments.

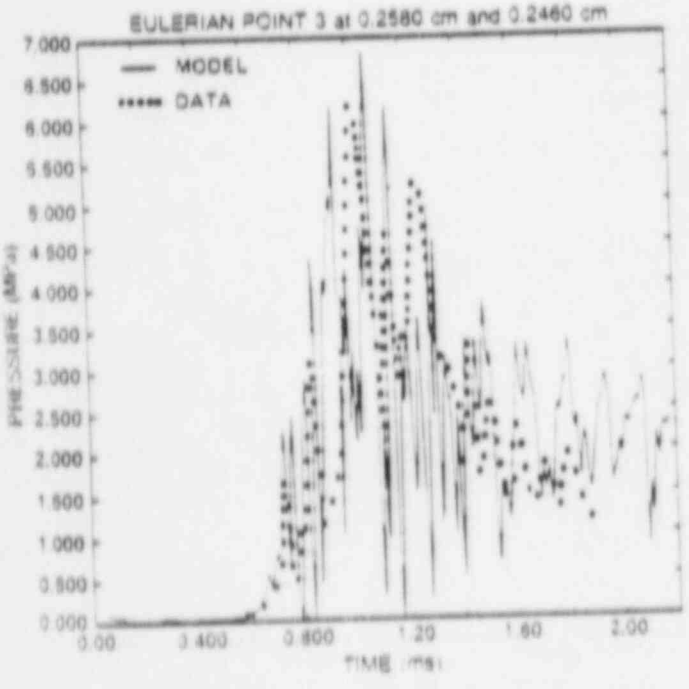

Fig. 10. Comparison of the calculation and the data for FITS test MD-19.

VI. CONCLUSIONS AND RECOMMENDATIONS

For the large-scale experiments, a transient one-dimensional explosion propagation model was developed and qualitatively predicted the FITS experimental data trends, e.g., pressure history and propagation velocity of the explosion. Phenomenological treatments for vapor film collapse and fuel fragmentation were incorporated into the model. In addition, a simple empirical explosion model was developed and incorporated into a two-dimensional hydrodynamic computer code, CSQ. This model has the unique capability of investigating the two-dimensional characteristics of the propagation and expansion phases of the explosion. It is being used to analyze the FITS experiments.

This paper has outlined new models that were employed to analyze the test data of large-scale experiments. These models, although much more sophisticated than their predecessors, are still quite elementary and rely upon empirically based constants in two key areas: (a) the dominant fuel fragmentation mechanism, and (b) the fraction of the water within the initial fuel-coolant mixture that is actually involved in the explosive heat transfer. These two quantities have not been directly measured during

a steam explosion experiment. It is in this area that further research is recommended. However, it should be recognized that this work, although important in understanding the physics of the interaction, may not directly affect reactor safety questions.

The second area of future work should address why Corium-A+R does not undergo a violent interaction with water. If it is due to solidification processes, then it depends on the temperature of the core melt. This suggests that more research be focused on the initial conditions of the core melt accident.

APPENDIX

ONE-DIMENSIONAL TRANSIENT EXPLOSION MODEL

The one-dimensional transient explosion model was developed to analyze the large-scale experiments of Mitchell. It is based on the conceptual picture of a multitude of molten fuel droplets in film boiling in a continuous phase of liquid coolant. The assumptions of the model are discussed in Sec. IV. In the Appendix, the governing equations for this multiphase system are presented, along with a couple of sample calculations.

The one-dimensional Lagrangian hydrodynamic wave code, WONDY-IV, was modified to incorporate this multiphase system and the assumed fuel fragmentation models (thermal and mechanical mechanisms). This wave code was designed to solve conventional continuum relations; however, it was easily modified for this problem.

The mass continuity equation is given by

$$\frac{d}{dt}(\rho_m x) = 0 \ , \tag{A.1}$$

where x is the one-dimensional position at a Lagrangian cell interface (Fig. A.1) and where ρ_m is the mixture density centered in the mesh cell

$$\rho_m = \rho_f \alpha_f + \rho_v \alpha_v + \rho_c \alpha_c \ , \tag{A.2}$$

where $\alpha_{f,v,c}$ are the volume fractions of the fuel, vapor, and liquid coolant, respectively, subject to the constraint

$$\alpha_f + \alpha_v + \alpha_c = 1 \ . \tag{A.3}$$

The volume fraction of fuel is simply the droplet volume divided by the mesh cell unit volume, Δx (Fig. A.2):

$$\alpha_f \equiv \frac{\frac{\pi}{6} D_f^3}{\Delta x^3} \ . \tag{A.4}$$

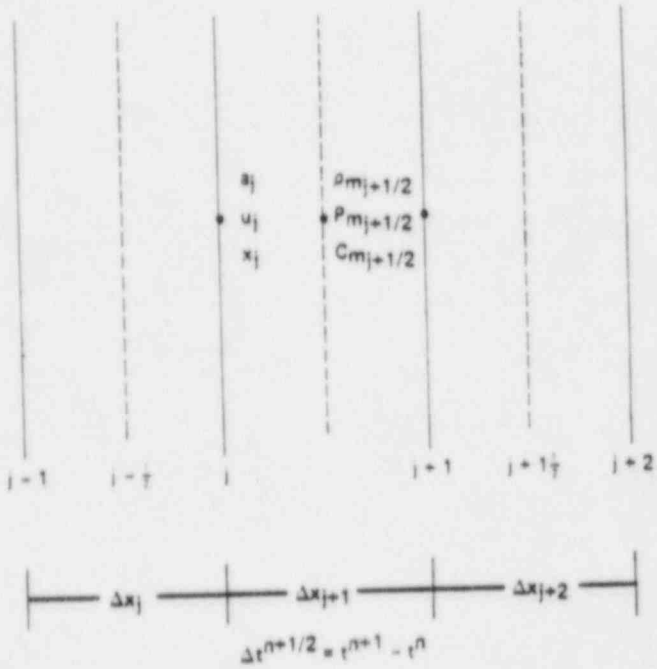

Fig. A.1. Spatial mesh for the one-dimensional Lagrangian model.

Similarly,

$$\alpha_v \equiv \frac{\frac{\pi}{6}[(D_f + 2\delta)^3 - D_f^3]}{\Delta x^3} \tag{A.5}$$

$$\alpha_c = 1 - \alpha_f - \alpha_v \ . \tag{A.6}$$

The one-dimensional momentum equation for rectangular coordinates is given by

$$\rho_m a = -\frac{\partial \sigma}{\partial x} - \frac{\partial q}{\partial x} \ , \tag{A.7}$$

where a is the acceleration at the cell interface,

$$a \equiv \frac{\partial U}{\partial t} \ , \tag{A.8}$$

and where

U = velocity at the cell interface

$$U \equiv \frac{\partial x}{\partial t} \tag{A.9}$$

σ = stress in the x direction, where for this multiphase fluid system is equal to the mixture pressure

$$\sigma \equiv P_m \tag{A.10}$$

q = viscous stress given by

$$q = B_1^2 \rho_m \Delta x \frac{1}{\rho_m}\left(\frac{\partial \rho_m}{\partial t}\right)^2 + B_2 c_m \Delta x \left(\frac{\partial \rho_m}{\partial t}\right) \tag{A.11}$$

and B_1 and B_2 are the quadratic and linear viscosity coefficients.

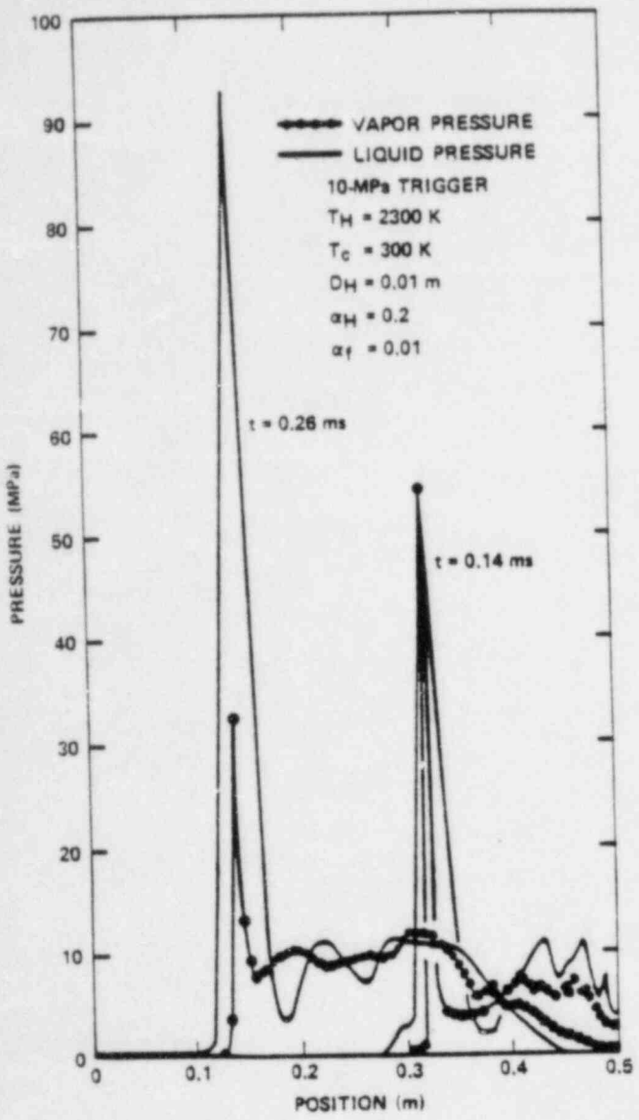

Fig. A.2. One-dimensional calculation using the mechanical fuel fragmentation mechanism.

Viscosity is included in the calculation because it causes shock waves in the fluid to have a finite slope in contrast to ideal inviscid theory. However, natural viscosity is so small that the shock width would still be extremely narrow requiring very fine zoning of the problem. Therefore, these artificially large viscosity coefficients are introduced for the express purpose of reducing shock gradients and spreading out the shock over a few mesh cells. For these multiphase explosion calculations, it was empirically found that these coefficients could be reduced at least an order of magnitude below recommended values without affecting the solution, because the multiphase system physically adds shock wave damping.

In WONDY the explicit finite difference algorithm solves these mass and momentum equations simultaneously in a mesh cell for new values of density, $\rho_m(t^{n+1})$, position, $x(t^{n+1})$, and velocity, $v(t^{n+1})$, using the old pressure values, $P_m(t^n)$, and internal energy, $E_m(t^n)$. Then the equations of state and conservation of energy are solved simultaneously for new values of $P_m(t^{n+1})$ and $E_m(t^{n+1})$. Only the equations of state and energy for the fuel, vapor, and liquid needed to be reformulated and included into the WONDY model. These field equations in this multiphase system are local statements for one particular numerical mesh cell; that is, they do not contain spatial gradients from neighboring mesh cells, and thus can be solved separately from mass and momentum.

TABLE A.I

Governing Equations for Film Collapse

Rayleigh equations for liquid:

$$\frac{dU}{dt} = \frac{1}{R_\delta}\left(\frac{p_f - p_\infty}{\rho_c} - \frac{3}{2}U^2\right) . \qquad \text{(A.I.1)}$$

Velocity of the vapor-liquid interface:

$$\frac{dR_\delta}{dt} = U + \frac{dm_v/dt}{4\pi R_\delta^2 \rho_c} . \qquad \text{(A.I.2)}$$

Energy equation for fuel:

$$\int_{R-\lambda_H}^{R} dr r^2 \frac{\partial T_H}{\partial t} = \alpha_H r^2 \frac{\partial T_H}{\partial r}\bigg|_{R-\lambda_H}^{R} . \qquad \text{(A.I.3)}$$

where

$$T_H - T_{HC} = (T_{HS} - T_c)\left\{1 - \left[\frac{(R-r)}{\lambda_H}\right]^2\right\} . \qquad \text{(A.I.4)}$$

Fuel-vapor boundary condition:

$$-k_H \frac{\partial T_H}{\partial r}\bigg|_R = -k_v \frac{\partial T_v}{\partial r} + \sigma_r(T_{H_s}^4 - T_v^4) . \qquad \text{(A.I.5)}$$

Energy equation for coolant liquid:

$$\int_{R+\delta}^{R+\delta+\lambda_c} dr\left(r^2 \frac{\partial T_c}{\partial t} + U\frac{\partial T_c}{\partial r}\right) = \alpha_c r^2 \frac{\partial T_c}{\partial r}\bigg|_{R+\delta}^{R+\delta+\lambda_c} , \qquad \text{(A.I.6)}$$

where

$$(T_c - T_{cl}) = \left[(T_f - T_{cl})\left(1 - \frac{x}{\lambda_c}\right)^2\right] ; \quad x = r + R + \delta . \qquad \text{(A.I.7)}$$

Coolant liquid-vapor boundary condition:

$$-k_c \frac{\partial T_c}{\partial r}\bigg|_{r=R+\delta} + \frac{dm_v}{dt} h_{fg} = -\frac{k_v \partial T_v}{\partial r}\bigg|_{r=R+\delta} + \sigma_r(T_{H_s}^4 - T_f^4) . \qquad \text{(A.I.8)}$$

TABLE A.II

Equilibrium and Nonequilibrium Models for the Vapor Film

Equilibrium

Energy equation for vapor:

$$\frac{d(m_v u)}{dt} = \dot{Q} - P_f \frac{dV}{dt} + \dot{m}_v h_{sat} \quad \text{(A.II.1)}$$

where

$$\dot{Q} = \frac{2k_v}{\delta}(T_I - T_v) + \frac{2k_v}{\delta}(T_{HS} - T_I) \quad \text{(A.II.2)}$$

$$u \equiv h - pv \quad \text{(A.II.3)}$$

$$h \equiv \frac{\gamma_c R_c}{\gamma_c - 1}(T_v - T_I) + h_{sat} \quad \text{(A.II.4)}$$

$$h_{sat} = h_{fg} + c_{P_c}(T_I - T_{ref}) + h_{ref} \quad \text{(A.II.5)}$$

$$T_I = T_{sat} \quad \text{(A.II.6)}$$

$$V = \frac{4}{3}\pi(R_\delta^3 - R^3) \quad \text{(A.II.7)}$$

$$P_f = P_g + P_{sat}(T_I) \quad \text{(A.II.8)}$$

Rate of evaporation:

$$\dot{m}_v = \frac{1}{h_{fg}}\left[\frac{2k_v}{\delta}(T_V - T_I) - \frac{2k_c}{\lambda_c}(T_I - T_c)\right] \quad \text{(A.II.9)}$$

Nonequilibrium

Energy equation for vapor:

$$\int_0^\delta \left(\rho_v \frac{\partial h}{\partial t} + U_v \frac{\partial h}{\partial x}\right)dx = k_v \frac{\partial T_v}{\partial x}\bigg|_0^\delta + \int_0^\delta dx \frac{\partial P_f}{\partial t} \quad \text{(A.II.10)}$$

where

$$x = R + r \quad \text{for } R \leq r \leq R + \delta \quad \text{(A.II.11)}$$

$$U_x = \frac{x}{\delta}\left(\frac{dR\delta}{dt}\right) \quad \text{(A.II.12)}$$

$$\rho_v = \frac{P_f}{RT_v} \quad \text{(A.II.13)}$$

$$T_v = T_{H_s} + (T_{g_v} - T_{H_s})\frac{x}{\delta} + C_T\left[\left(\frac{x}{\delta}\right)^2 - \frac{x}{\delta}\right] \quad \text{(A.II.14)}$$

$$C_T = \frac{-Me}{A}\left(\frac{\gamma_c R_c}{\gamma_c - 1}\right)(T_{g_v} - T_{c_v})\left(\frac{\delta}{k_v}\right) + T_{H_s} - T_{c_v} \quad \text{(A.II.15)}$$

Rate of evaporation:

$$\dot{M}_v = 4\pi R_\delta^2\left(\frac{M_e}{A} - \frac{M_c}{A}\right) \quad \text{(A.II.16)}$$

$$\frac{M_e}{A} = \frac{\sigma_A P_{sat}(T_{c_v})}{(2\pi R_c T_{c_v})^{1/2}} \quad \text{(A.II.17)}$$

$$\frac{M_c}{A} = \frac{\sigma_A P_{sat}(T_{g_v})}{(2\pi R_c T_{g_v})^{1/2}} \quad \text{(A.II.18)}$$

For modeling the film collapse phase of the explosion, given a trigger pulse, the models used in analyzing Nelson's small-scale tests[4] were incorporated into WONDY (see Tables A.I and A.II). In particular, the equilibrium film collapse model was used in the calculations presented in Sec. IV. Note that there is a local momentum equation included in the analysis that accounts for inequality of liquid and vapor pressures due to dynamic effects.

For modeling the explosion phase of a single fuel droplet after local film collapse has been predicted to occur, the thermal fuel fragmentation model or the mechanical fuel fragmentation model[22] was used.

The governing energy and state equations for both the film collapse and droplet fragmentation-explosion phases were included into WONDY as a subroutine, which is called for each mesh cell after the mass and momentum equations are solved. To accomplish this, the old and new values of density, ρ_m, in a mesh cell were linearly interpolated to give a continuous value of ρ_m across a time step:

$$\rho_m(t) = \rho_m(t^n) + \frac{\rho_m(t^{n+1}) - \rho(t^n)}{t^{n+1} - t^n}\, t \quad \text{(A.12)}$$

Then the energy and state equations for the fuel, vapor, and liquid coolant were considered as a system of nonlinear ordinary differential equations with time as the independent variable and were numerically integrated using a Runge-Kutta technique from t^n to t^{n+1}. This method provides new values of all the variables at t^{n+1}. From this, a new value of mixture pressure, P_m, and energy, E_m, for the mesh cell are saved for the next calculation of mass and momentum. For the calculations presented here, the mixture pressure was taken to be that of the liquid coolant, P_c, because it is the continuous fluid in the calculation.

NOMENCLATURE

a = acceleration

A_p = projected area

A_d = droplet surface area

c = heat capacity (subscripts: p = constant pressure and v = constant volume)

D = diameter

h = enthalpy

h_{fg} = latent heat of vaporization

h_{ref} = reference enthalpy

h_{TOT} = heat transfer coefficient

k = thermal conductivity

m_v = coolant mass vaporized at interface
m = mass
M_{slug} = liquid slug mass
P = pressure
P_∞ = ambient pressure
P_g = noncondensable gas pressure
ΔP_{con} = pressure due to fuel-coolant contact and mixing
$\dot{q}$ = heat transfer rate
r = radius
R_f = radius of fuel drop
R_v = radius of vapor-liquid interface
R = gas constant for water
t = time
u = internal energy
U = velocity
V = volume
V_b = (expansion) volume
V_e = entrained volume
v = specific volume
X = quality
x = distance or position
α = volume fraction
δ = vapor film thickness
δ_c = condensate thickness
γ = ratio of specific heats
λ_c = coolant thermal penetration distance
λ_f = fuel thermal penetration distance
λ_{crit} = Taylor critical wavelength
ρ = density
σ = surface tension
σ_A = accommodation coefficient
σ_r = Stefan-Boltzmann constant

Subscripts

c = coolant
e = equilibrium
f = fuel
i = initial
rel = relative
v = coolant vapor
t = trigger